

Gluon Emission of Heavy Quarks: Dead Cone Effect

R. Thomas¹, B. Kämpfer¹, G. Soff²

¹ Forschungszentrum Rossendorf, PF 510119, 01314 Dresden, Germany

² Institut für Theoretische Physik, TU Dresden, 01062 Dresden, Germany

Received ...

Abstract. The lowest-order induced soft gluon radiation processes of heavy quarks have been analyzed to quantify the dead cone effect. This effect is most likely expected to suppress significantly the energy loss of charm quarks passing an amorphous color-neutral deconfined medium, as has been concluded from recent experiments at RHIC.

Keywords: Induced gluon radiation, energy loss, dead cone

PACS: 25.75.-q, 11.10.10.Wx

1. Introduction

Radiative energy loss of quarks traversing strongly interacting matter is considered as a promising probe of the quark gluon plasma. Indeed, the recent heavy-ion collision experiments at RHIC show a distinct suppression of transverse momentum spectra of hadrons composed of light quarks [1] thus evidencing the transient creation of a medium with large stopping power caused by a high gluon density. In contrast, open charm mesons [2] seem to suffer only a tiny, if any, energy loss [3]. As noted in [4] prior to this experimental finding, the gluon emission pattern of heavy quarks experiences a modification, known from jet physics as dead cone effect, which reduces the radiative energy loss. While large efforts are devoted to the study of the energy loss of light quarks at asymptotic energies (cf. [5, 6, 7, 8, 9, 10, 11, 12, 13] and further references therein), the treatment of heavy quarks [14, 15] is in progress.

Similar to the fairly complete treatment of the radiative energy loss of light high-energy quarks we consider here the lowest-order induced gluon emission of a heavy quark. It is our goal to take exactly into account the finite mass, the finite energy and correct kinematics (i.e. not only soft gluon emission), the full color algebra and all spin/polarisation effects. In doing so we restrict ourselves to the single scattering and one-gluon emission process. The importance of the single scattering

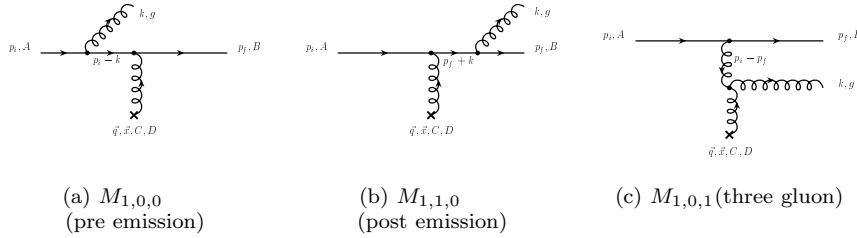


Fig. 1. Diagrams of single scattering with one-gluon emission classified by the notation scheme $M_{n,m,l}$ of [6].

process is emphasized by various aspects. Among of them data from RHIC, which suggest thin plasmas, imply that only a few scatterings are taking place; single scattering is the first, and according to [7] the most important. The existence of an analogue to the Landau-Pomeranchuk-Migdal (LPM) effect in QCD, which reduces the effective number of scatterings further, is another indication of the significance of this process. Moreover the fast convergence of the opacity expansion [7], where the first order describes the radiative energy loss considerably well, suggests the relevance of this basic energy loss process. The discussion of the QCD analog of the Ter-Mikaelian (TM) effect [16] is also based on the lowest order in opacity [17]¹.

The article is organized as follows. In Section 2 we describe the potential model and the concept of radiation amplitude and dead cone factor. Numerical results are then discussed in Section 3. The validity of the potential model is commented on in Section 4. The last part summarizes conclusions.

2. Single Scattering in the Potential Model

Following [19] we consider the processes depicted in Fig. 1. The crosses stand for external potentials which, according to [13], represent the medium. A color charge, here a quark, moving through a background field of quarks and gluons is mimicked by scattering on target particles modeled by static screened potentials

localized at the space points \vec{x}_i , $V_{AB}^a(\vec{q}) = gT_{AB}^a \frac{e^{-i\vec{q}\vec{x}_i}}{\vec{q}^2 + \mu^2}$, \vec{q} is the momentum transfer and μ is the Debye screening mass; the coupling g is not varying here. The term $T_{AB}^a = \chi_B^\dagger C_{b_1 \dots b_n}^{a_1 \dots a_m} \chi_A$ stands for the original color structure of the target, where T^a are generators of $SU(3)_{color}$, χ the quark color states and $A, B = 1 \dots 3$ are color indices. In order to allow for the neglect of radiation contributions from targets in the realistic situation where the potential in Fig. 1 is substituted by a dynamical target, and thus for a realistic model, one requires a particular gauge

¹The results of [17] confirm the conjecture [16] that the asymptotic gluon mass, which is also important for describing phenomenologically the quark-gluon plasma [18], determines the TM effect.

choice, the A^+ -gauge. The gauge choice is given by the condition $A^+ \equiv A^0 + A^z = 0$ in light-cone coordinates.

In the soft radiation limit the conditional probability of one-gluon emission under the condition that an elastic scattering has occurred is given by the ratio of the inelastic and elastic differential cross sections

$$dP = \frac{\overline{d\sigma_{\text{inel}}}}{\overline{d\sigma_{\text{el}}}} = \frac{\overline{|M_{\text{inel}}|^2}}{\overline{|M_{\text{el}}|^2}} \frac{d^3k}{2\omega(2\pi)^3}, \quad (1)$$

where the overline indicates an average over initial polarization and color configurations and a sum over all final polarizations and colors. Thus the sufficient quantity to compare different radiation patterns in such scattering processes is the radiation amplitude $\overline{|R|^2} = \overline{|M_{\text{inel}}|^2}/\overline{|M_{\text{el}}|^2}$. If the momentum of the gluon is small, compared to the momenta of the other particles, a factorization into a part describing the emitted radiation and an underlying part for the elastic scattering can be carried out on the level of the matrix elements.

The probability, i.e. the radiation amplitude, for gluon emission off heavy quarks in projectile direction is strongly reduced at radiation angles $\theta < \theta_0$ by a dead cone suppression factor according to F^2 [4] with

$$F = \frac{k_{\perp}^2}{k_{\perp}^2 + \omega^2\theta_0^2} = \frac{\sin^2\theta}{\sin^2\theta + \theta_0^2}, \quad (2)$$

which corrects the matrix elements derived in the approach of Gunion and Bertsch [19] for massless, high energetic quarks. Below $\theta_0 \equiv m/E$, where E means the energy of the incident heavy projectile quark, radiation becomes suppressed due to the mass m of the projectile, which introduces a new scale relevant for the radiation pattern. However, the suppression factor F is restricted to small angles. Moreover, this estimate is valid for soft gluons, that means it focuses on abelian diagrams only, and cannot properly handle intermediate gluon energies. These shortcomings can be overcome only by a numerical computation, which is the main motivation for the present work.

3. Numerical Results

The graphical elements depicted in Fig. 1 correspond to objects in our C++ code [20]. Therefore, the matrix elements are evaluated numerically. All interference effects are exactly dealt with when squaring sums of matrix elements and performing averaging/summation over spins/polarisations. Since spinor calculations do not reveal significant modifications we present results of the scalar QCD case and comment later on spin effects.

3.1. Abelian Region

To highlight the role of the non-abelian diagram 1c with the triple gluon vertex we consider first the "abelian part of QCD". In Fig. 2 the radiation amplitude obtained

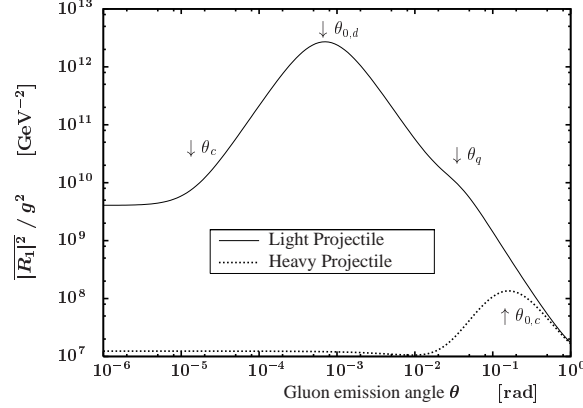


Fig. 2. Radiation amplitude $\overline{|R_1|^2}$ as a function of θ for $m < |\vec{q}_\perp|$ (light projectile quark, $m_d = 0.007$ GeV) and $m > |\vec{q}_\perp|$ (heavy projectile quark, $m_c = 1.5$ GeV). Radiation is suppressed for $\theta < \theta_0$ due to the dead cone effect, whereby the reduction is stronger as the quark mass grows. The chosen parameters are $\vec{p}_i = (0, 0, 10)$ GeV, $\vec{p}_{f\perp} = (0.3, 0.2)$ GeV, $\mu = 0.5$ GeV, and $\omega = 0.001$ GeV, $\phi = \pi/2$ for the emitted gluon.

from the abelian total matrix $M_{1,\text{rad}}^{\text{abel.QCD}} = M_{1,0,0}^{\text{QCD}} + M_{1,1,0}^{\text{QCD}}$ is shown as a function of the gluon emission angle θ , which encloses the directions of the gluon and the incident quark. For the same kinematics the cases of a light and a heavy projectile are contrasted and reveal significant suppression of the radiation pattern at angles $\theta < \theta_0$, which is the dead cone effect. The heavy particle case is classified with the condition $|\vec{q}_\perp| < m$, and vice versa, hence it depends on the choice of the transverse momentum transfer \vec{q}_\perp .

From analytical and approximated matrix elements one can derive the $1/(\omega^2\theta^2)$ decrease of the radiation amplitude for $\theta > \theta_0$ and a θ^2/ω^2 slope for $\theta < \theta_0$, as can be seen in Fig. 2 for both cases. This behavior for $\theta \sim \theta_0$ agrees with the dead cone factor.

Some additional features seen in Fig. 2 are clarified in Fig. 3, where the individual contributions for the light quark situation are depicted, including the non-abelian contribution. For angles θ between $\theta_q \equiv \frac{|\vec{q}_\perp|}{E}$ and $\theta_c \equiv \frac{m^2}{|\vec{q}|E} = \frac{\theta_0^2}{\theta_q^2}$ the pre-emission diagram dominates, and for $\theta > \theta_q$ pre- and post-emission interfere to yield a different color factor which accounts for the shift by $\frac{4}{9}$ at θ_q in Fig. 2. The constant post-emission process for $\theta < \theta_c$ determines the constant radiation amplitude in this angular region.

Although in Fig. 2 the picture of the radiation amplitude in the heavy quark case appears quite similar, here it is the pre- and post emission which interfere

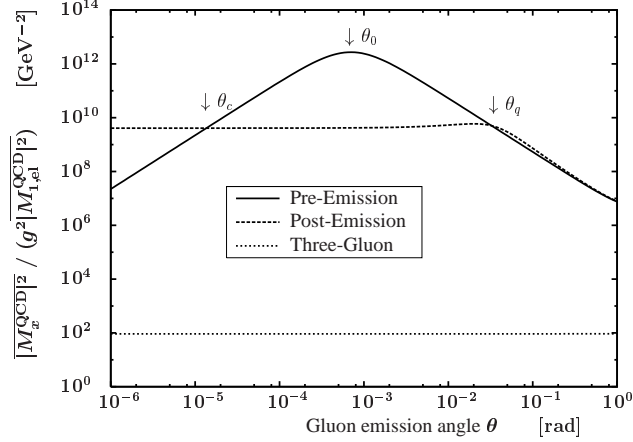


Fig. 3. Contributions of individual diagrams to the total results in Fig. 2 for the light quark scenario. The three-gluon contribution is suppressed by orders of magnitude and so the full QCD result does not deviate from the abelian QCD radiation amplitude.

with a magnitude of same order to obtain the dead cone behavior for $\theta_q < \theta$. The post-emission is dominant and constant for $\theta < \theta_q$ and thus the radiation amplitude becomes constant as well.

Note, that in a corresponding QED situation the radiation probability will be further reduced for $\theta > \theta_q$ due to destructive interference, which in QCD is excluded by color factors.

3.2. Non-Abelian Diagram and Factorization

We continue to discuss to which degree the three-gluon vertex diagram 1c contributes and how it may change the behavior of the abelian QCD single scattering radiation amplitude. In fact, the results for the kinematical situations considered so far for abelian diagrams are not effected by the additional three-gluon vertex diagram. Figure 2 is not modified by this contribution; its smallness is demonstrated for the light quark case in Fig. 3.

It can be shown that the non-abelian part becomes especially important for angles $\theta > \theta_{3glu}$ with $\theta_{3glu} \equiv \frac{|\vec{q}_\perp|}{\omega}$, but this implies $|\vec{q}_\perp| < \omega$, in order to consider such an angular configuration. This is for example realized in Fig. 4 where calculations of individual contributions in the heavy quark case are shown. It exhibits that the three-gluon contribution dominates in the whole θ range. However, if one allows for $\theta_{3glu} < 1$, this means to abandon the soft radiation limit. In other words, the condition $|\vec{q}_\perp| < \omega$ implies that the momentum transfers, which are constrained by initial and final states, differ significantly in the radiation and elastic scattering

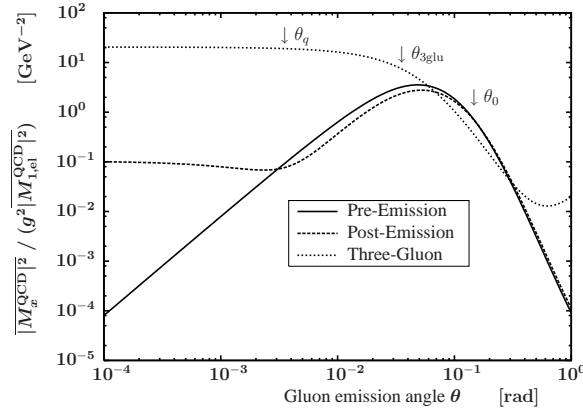


Fig. 4. Contributions of individual diagrams for a situation with a dominating three gluon vertex diagram. The parameters are chosen for $\theta_{3\text{glu}} < 1$, so that $\theta_{3\text{glu}} < \theta$ is possible, $m_c = 1.5$ GeV, $\vec{p}_i = (0, 0, 10)$ GeV, $\vec{p}_{f\perp} = (0.03, 0.02)$ GeV, $\mu = 0.05$ GeV, $\omega = 1$ GeV, $\phi = \pi/2$.

processes. But the latter serves as reference system for the definition of the radiation amplitude. The factorization, which is usually applied in the derivation of approximated matrix elements, becomes insufficient. In specific examples, this may be accounted for by an additional correction factor [20]. Here we mention that this problem causes e.g. θ_0 in Fig. 4 to be shifted off the peak position.

4. Validity of the Potential Model

It is tempting to test the validity of the potential model beyond the assumptions of massless scattering particles. We analyse this while we contrast the scattering of an incident particle in the potential model with an analogue scattering of the same projectile on a target quark at rest.

It was found that the radiation amplitude calculated in a quark-quark collision coincides well with the potential model result as long as the angles θ are small and the projectile is not heavier than the target.

The results of a scalar QCD calculation for light targets and heavy projectiles are exhibited in Fig. 5. There the radiation amplitude in the potential model can be well-described by the application of a general dead cone factor, which is valid for arbitrary angles. For smaller θ the potential model result becomes constant (cf. Fig. 2) and a simple dead cone factor does not longer apply. The dead cone suppression is weaker in a quark-quark scattering approach. This shows that for such an arrangement of colliding masses the potential model might be challenged, since the assumption, that no energy would be transferred to the target, is violated.

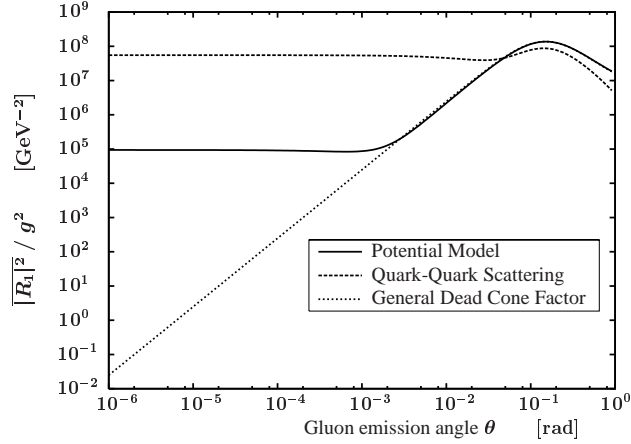


Fig. 5. The radiation amplitude $|R_1|^2$ as a function of the emission angle θ is compared for the potential model, the quark-quark scattering on a light target and the general dead cone factor. The chosen parameters are $m_d = 0.007$ GeV (light quark), $m_c = 1.5$ GeV (heavy quark), $\vec{p}_i = (0, 0, 10)$ GeV, $\vec{p}_{i, \text{Target}} = (0, 0, 0)$, $\vec{q}_\perp = (0, 0.01)$ GeV, $\mu = 0$, $\omega = 0.001$ GeV, $\phi = 3\pi/2$.

This is intended to possibly point to the need of an improved model to describe the scattering processes in a deconfined medium for heavy projectile quarks.

Besides this we have numerically justified the usual neglect of radiation contributions from the target lines in the A^+ -gauge. Also comparisons of scalar and spinor calculations did not reveal significant differences for small angles, light quarks and soft gluons.

In the light quark scattering we find only configurations without spin flip to contribute to the radiation amplitude. In contrast, scattering a heavy on a light quark revealed that configurations become important where the spin of the light target is flipped.

5. Conclusions

This work is aimed investigating how the mass parameter of an on-shell quark passing a deconfined medium influences its radiative energy loss probability. A detailed discussion of the basic single scattering diagrams with one-gluon emission in the potential model was done. With the numerical calculation of the radiation amplitude in QCD we could disentangle interference effects, especially the influence of the non-abelian effects.

The dead cone suppression factor was shown to emerge in specific angular regions, however the radiation amplitude deviates from this prediction for either small angles, due to the post-emission process, or in case of higher gluon energies ω . For

the latter possibility the three-gluon diagram, including the three-gluon vertex, becomes responsible. We thus have confirmed the suppression effect due to the heavy quark mass, but find the dead cone factor (2) is not the correct modification in all kinematical situations. (This finding agrees with the one in [14], where an averaged dead cone suppression factor was also found to be insufficient.) We stress that not the mass parameter of the projectile itself but the ratio to the transverse momentum transfer is relevant to categorize light and heavy mass situations. Non-abelian effects become important for large gluon energies, that is to say greater than the transverse momentum transfer.

We have indicated that the potential model might become inappropriate if heavy projectile quarks are present. In addition, it was emphasized that for considerably large values of the gluon energy one is confronted with factorization problems with respect to the elastic scattering part in matrix elements. In such situations the missing unique interpretation of the radiation amplitude questions whether it is sufficient to consider ratios of inelastic and elastic cross sections.

The numerical confirmation of the LPM effect and the calculation of net energy loss of heavy quarks at finite energy along the lines of [14, 15] are promising goals of further investigation, such as the extension of our approach to multiple scattering, i.e. higher orders in opacity, and multi-gluon emission.

Acknowledgement(s)

Enlightening discussions and guidance of O.P. Pavlenko are gratefully acknowledged. The work is supported by BMBF 06DR121 and GSI.

References

1. K. Adcox et al. (PHENIX), *Phys. Rev. Lett.* **88** (2002) 022301, **91** (2003) 072303; C. Adler et al. (STAR) *Phys. Rev. Lett.* **89** (2002) 202301, **90** (2003) 082302; B.B. Back et al. (PHOBOS), *Phys. Rev. Lett.* **91** (2003) 072302.
2. K. Adcox et al. (PHENIX), *Phys. Rev. Lett.* **88** (2002) 192303.
3. K. Gallmeister, B. Kämpfer, *Nucl. Phys. A* **715** (2003) 705.
4. Y.L. Dokshitzer, D. E. Kharzeev, *Phys. Lett. B* **519** (2001) 199.
5. R. Baier et al., *Nucl. Phys. B* **483** (1997) 291, **484** (1997) 265, *Phys. Rev. C* **58** (1998) 1706, *JHEP* **109** (2001) 033.
6. M. Gyulassy, P. Levai, I. Vitev, *Nucl. Phys. B* **571** (2000) 197.
7. M. Gyulassy et al., *Phys. Lett. B* **243** (1990) 432, *Phys. Rev. Lett.* **85** (2000) 5535, **86** (2001) 2537, *Nucl. Phys. B* **594** (2001) 371, *Phys. Rev. D* **66** (2002) 014005.
8. C.A. Salgado, U. Wiedemann, *Phys. Rev. Lett.* **89** (2002) 09230, **68** (2003) 014008, U.A. Wiedemann, *Nucl. Phys. B* **588** (2000) 303, **582** (2000) 409.
9. P. Arnold, G.D. Moore, L.G. Yaffe, *JHEP* **0206** (2002) 030.
10. B. Müller, *Phys. Rev. C* **67** (2003) 061901.

11. X.N. Wang et al, *Phys. Rev. Lett.* **68** (1992) 1480, **77** (1996) 231; X.N. Wang, *Phys. Rev. C* **63** (2001) 054902, *Phys. Lett. B* **579** (2004) 299; X.F. Guo, X.N. Wang, *Phys. Rev. Lett.* **85** (2000) 3591; E. Wang, X.N. Wang, *Phys. Rev. Lett.* **89** (2002) 162301.
12. R. Baier et al., *Ann. Rev. Nucl. Part. Sci.* **50** (2000) 37; A. Kovner, U.A. Wiedemann, hep-ph/0304151.
13. M. Gyulassy, X.N. Wang, *Nucl. Phys. B* **420** (1994) 583; X.N. Wang, M. Gyulassy, M. Plümer, *Phys. Rev. D* **51** (1995) 3436.
14. N. Armesto, L.A. Salgado, U.A. Wiedemann, hep-ph/0312106.
15. M. Djordjevic, M. Gyulassy, *Nucl. Phys. A* **733** (2004) 265.
16. B. Kämpfer, O.P. Pavlenko, *Phys. Lett. B* **477** (2000) 171.
17. M. Djordjevic, M. Gyulassy, *Phys. Lett. B* **560** (2003) 37, *Phys. Rev. C* **68** (2003) 034914.
18. A. Peshier et al., *Phys. Rev. D* **54** (1996) 2399, *C* **61** (2000) 045203, *D* **66** (2002) 094003.
19. J. F. Gunion and G. Bertsch, *Phys. Rev. D* **25** (1982) 746.
20. R. Thomas, *Diploma Thesis*, TU Dresden 2003.